TINKER

FABRICATION OF SENSOR PACKAGES ENABLED BY ADDITIVE MANUFACTURING

= Deliverable D5.3 =

Prototype of NIL resist with high refractive index

This project has received funding from the European Union's Horizon 2020 research and innovation programme under the Grant agreement n°958472, project TINKER.

DT-FOF-07-2020
Assembly of micro parts (RIA)

TINKER

FABRICATION OF SENSOR PACKAGES ENABLED BY ADDITIVE MANUFACTURING

Starting date of the project: 01/10/2020
Duration: 36 months

= Deliverable D5.3 =

Prototype of NIL resist with high refractive index

Due date of deliverable: 31/12/2021
Actual submission date: 17/01/2022

Responsible WP: Michael Haslinger, WP5, PROFACTOR GmbH
Responsible TL: Jukka Perento, INKRON
Revision: V1.2

AUTHOR

Author	Institution	Contact (e-mail, phone)
Mikko Poutanen	IKR	mikko.poutanen@inkron.com, +358415482700
Jukka Perento	IKR	jukka.perento@inkron.com, +358405910419

DOCUMENT CONTROL

Document version	Date	Change
V1.0	08.11.2021	Draft template prepared
V1.1	08.12.2021	Deliverable report
V1.2	15.12.2021	Reviewed draft version

VALIDATION

Reviewers		Validation date
Task Leader	Jukka Perento	8.12.2021
Work Package Leader	Michael Haslinger	22.12.2021
Coordinator	Leo Schranzhofer	15.01.2022

DOCUMENT DATA

Keywords	
Point of Contact	Name: Mikko Poutanen Partner: Inkron Oy Address: Kutojantie 2 A 02630 Espoo FINLAND Phone: +358415482700 E-mail: mikko.poutanen@inkron.com
Delivery date	8.12.2021

Executive Summary

This deliverable report summarizes the properties of a prototype material, IPO-912, which is an ink jet compatible and nanoimprintable resist with refractive index (n_D) of 1.9 and has been developed to act as a functional material in the waveguides of the optical phase arrays of the LIDAR sensor demonstrators in TINKER. As a key feature, the resist has a high refractive index and it is developed to be compatible with inkjet printing as an application method. Inkjet printing of the high refractive index resist allows for digital deposition of the material specifically to locations where it's needed. Additionally, it allows for variation of the layer thickness to accommodate for the varying volume filling in the structures.

The report presents the main physical properties of IPO-912, demonstrates its ink jetting and nanoimprinting properties, first separately, and then as a combination.

The resist fulfils the definitions for the prototype material as specified for the deliverable. As the following development steps, the prototype material will be distributed to the respective consortium partners for further process testing. During development, the resist properties have been chosen to allow for modifications affecting the nanoimprintability and ink jet properties separately. This aims at allowing control of the material thickness range at varying ink jet conditions, control of ink jet patternability and further improvements of the nanoimprinting and optical properties as subsequent development versions.

Table of Contents

1. Introduction

The vision of TINKER is to provide a new cost- and resource efficient pathway for RADAR and LIDAR sensor package fabrication with high throughput up to 250units/min, improved automation by 20%, improved accuracy by 50% and reliability by a factor of 100 to the European automotive and microelectronic industry via additive manufacturing and inline feedback control mechanisms. Autonomous driving and self-driving cars represent one prominent example for the use of microelectronics and sensor, most importantly RADAR and LIDAR sensors. Their respective markets have a big potential, e.g. it is estimated that the market size of LIDAR in automotive will double itself in the next two years (within 2020 to 2022).

Figure 1: TINKER overview

The public awareness and the industrial need for further miniaturization of such sensor packages is the main driver of ongoing efforts in the automotive sector to be able to integrate such devices into the car body like in the bumpers and head lamps instead of attaching them (e.g. on top of the car in case of LIDAR device). Safety (for the driver and others) is the most important key aspect of the automotive sector. Therefore, high-value and high performance RADAR and LIDAR systems are required for advanced driver-assistance systems (ADAS) as well as robotic cars. Current bottlenecks are the relatively large size of such sensor devices, their weight and power consumption. Since these factors are highly limited within cars, further miniaturization and improving functionality and efficient use of resources is highly demanded.

1.1. Description of deliverable

The deliverable D5.3 is a prototype of a material with a high refractive index as defined in the deliverables D2.2 and D2.5. The refractive target for the functional resin has been agreed to be 1.9 (n_D) during the project. The application method for the material was chosen to be inkjet printing to allow for digital deposition of the material in specific locations on the substrates.

The definition of deliverable D5.3 also states materials on the pathway towards the RI 1.9 ink jet compatible NIL resist. This pathway includes for example a refractive index 1.7 ink jettable material – named as IPO-711 – which is not reported here.

2. Results and Discussion

2.1. Ink formulation

Inkron high refractive index (RI) resins are based on utilizing nano-sized fillers to increase the refractive index of the samples. The high refractive index nanoimprint resin comprises mainly of 1) resin, 2) nanofillers, 3) solvent system and 4) additives. There are several key properties required from the ink jettable prototype material to work in an optical application with NIL processing. The main properties are:

- Optical properties (refractive index, low internal losses)
- Nanoimprintability (patternability, pattern fidelity, process stability)
- Ink jet properties (stable ink jetting, patternability, layer thickness)
- Product stability and compatibility

These properties have been optimized during the product development by adjusting the composition. The formulation is developed to allow further changes to tune the prototype material system for different purposes and processing with different printheads. From the formulation components, the two former materials are the main factors determining the imprinting properties, whereas within specific constraints, the solvent system has minimal effect on the imprinting properties. Therefore, especially the solvent system and additives are used to adjust the ink jetting properties.

2.2. Ink properties

IPO-912 is formulated to allow its deposition via ink jet printing. The viscosity, surface tension and solid content are presented in The surface tension of the resist is 32 mN/m, which is suitable for ink jetting.

Table 1. The solid content of the prototype material as described here is 48 w-%. At this solid content, and the used solvent system, the viscosity between 25°C and 40°C ranges between 18.9 and 12.1 mPa.s, respectively. The viscosity is mostly a function of the solvent system and the solid contents, as seen necessary for various purposes and within certain constraints, the viscosity can be adjusted for example to affect the final layer thickness with specific ink jetting conditions. The surface tension of the resist is 32 mN/m, which is suitable for ink jetting.

Table 1. Basic properties of prototype material of IPO-912

Viscosity, mPa.s	at 25°C	18.9
	at 30°C	16.1
	at 35°C	13.9
	at 40°C	12.1
Surface tension, mN/m		32
Solid content, w-%		48

IPO-912 is a UV-curable material, developed to be cured with high intensity 365 nm UV-LED illumination. The UV intensity during testing in the development phase has been 200-500 mW/cm^2, which is compatible with the UV exposure intensities in EVG SmartNIL tooling. The curing of the resist is partially oxygen inhibited, but the curing process is designed and tested to work under the working stamp foils of the nanoimprint tooling. For first tests, 20 J/cm^2 is suggested as the curing dose, but the dosage can be decreased during process optimization.

The IPO-912 material is formulated with TiO_2 nanofillers to increase the refractive index of the resist. Generally, the RI is tuned by the resin and nanofiller loading. In this project, the target is to increase the refractive index as high as possible while retaining sufficient nanoimprinting properties to allow imprinting of the photonic integrated structures. A significant amount of work has been used to optimize the nanofiller properties to achieve good imprintability in combination with good optical properties.

The refractive index of the cured resist is depicted in Figure 2 as measured via ellipsometry. The refractive index is measured from ink jetted film with a thickness of 235 nm. The refractive index n_D (at 589 nm) of the prototype reported here is 1.92, which leads to a refractive index of 1.85 at 1550 nm as extrapolated from the measured data.

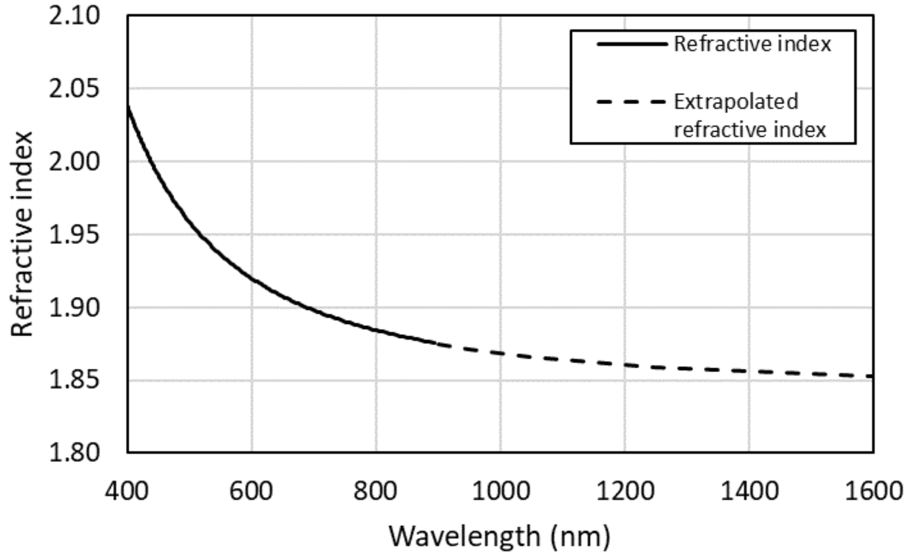

Figure 2. The refractive index of the cured IPO-912 prototype material as measured from an inkjetted film with thickness of 235 nm.

One of the most important properties for the resin are its optical properties, namely transmittance and haze induced by the nanofillers of the resin. The transmittance spectrum of a resist creating a similar cured film as IPO-912 is depicted in Figure 3. The film was deposited by spin coating onto an index matching glass with a refractive index (n_D) 1.9 and thickness of 500 µm. The film thickness was measured to be 776 nm. The transmittance measurement of the substrate is shown as a reference. The data shows that the transmittance of the resist is on a similar level as the transmittance of the substrate throughout the wavelength spectrum. Despite the index matching at n_D, the data of the resist shows interference pattern. The interference arises from the different optical dispersion properties. The measurement includes the surface reflections as losses, and therefore matching with the substrate indicates that there are no measurable absorptive/scattering losses except at <500nm.

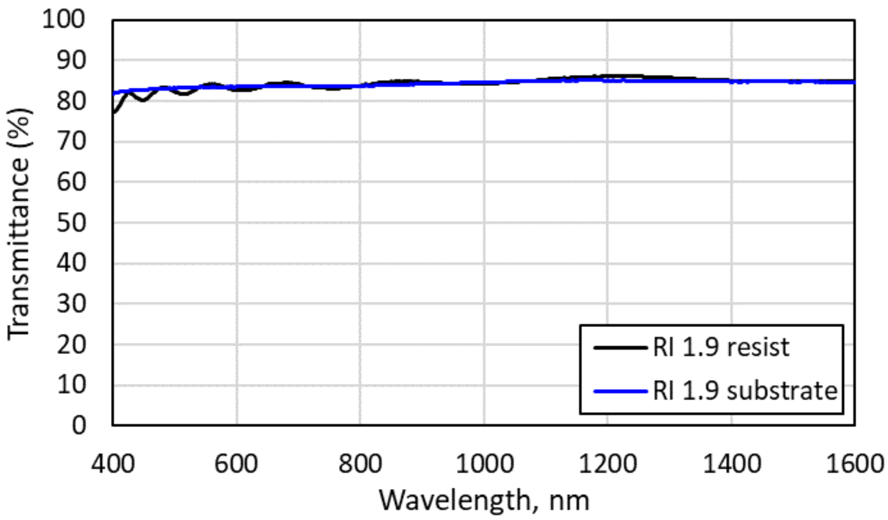

Figure 3. Transmittance of visible and NIR light of a resist with refractive index of 1.9 as a 776 nm thick layer on a glass substrate with a refractive index (n_D) of 1.9.

2.3. Ink jet properties

As a digital deposition technique, the key properties for the inkjet material are stable drop formation, patternability and thickness control and uniformity. These properties have been studied during the development of the materials. Additionally, the material stability in the ink jetting process has proven to be a constraint for the ink formulation. Specifically, the flowability of the resin needs to be retained for nanoimprinting and the optical quality of the ink jetted films needs to be ensured. As an example, specific components – usable in spin coated films – can cause a significant increase in the haze values of the ink jetted film.

The ink jetting properties of IPO-912 were investigated mostly using PIXDRO LP50 ink jet printer with Samba DMC 2.4 pl cartridges. The optimal viscosity range of the Samba cartridge is 4-8 mPa.s and the surface tension range is 28-32 dynes/cm. The native resolution of the printhead is 75 dpi and therefore multiples of the 75 dpi were used. The layer thickness target of IPO-912 was set at 200 nm during development, and to reach this value with the DMC 2.4 pl printheads, a high solids content sample was used. IPO-912 prototype formulation as reported here is on the upper limit of the viscosity range for the DMC 2.4 pl printheads used. As is reported in Table 1, the viscosity of IPO-912 is 16.1 mPa.s at 30°C, which is outside the recommended range, but the ink still inkjets for the testing purposes. Figure 4 shows an example of the ink droplets as observed in dropview of the ink jet printer. On other printheads, like XAAR 1003, the viscosity range is different, but so is the drop volume, likely leading to adjustments in the solids content of the formulation to reach the specific thickness range needed.

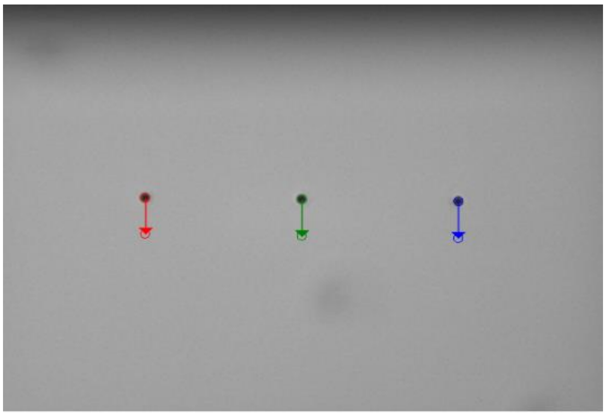

	v (m/s)	V (pl)	X (µm)	Y (µm)	Angle (°)
→	3.32	± 3.8	311	462	0.00°
→	3.37	± 3.5	648	465	0.00°
→	3.40	± 3.3	987	470	-0.13°

Figure 4. An example from the drop-view image of IPO-912 with the Dimatix DMC Samba 2.4 pl printhead on the PIXDRO LP50 inkjet printer. The drop volume and speed are subject to change with the different inkjetting parameters.

The patternability, and specifically the levelling behaviour of the films was investigated. Figure 5 shows examples of ink jetted squares at different conditions. The ink jetting was done on Si wafers primed with an adhesion promoter – IAP-110, which is the recommended adhesion promoter for Inkron high-RI materials. The arrays of droplets show that the ink jetting is stable and that the droplets are of uniform size and uniformly distributed. The ink jetted square patterns show good thickness uniformity at low thicknesses as ink jetted at 450 dpi. If the dpi values are increased, the wet layer thickness of the ink jetted film increases so that the resin layer starts to flow over larger distances. This can deteriorate the layer thickness uniformity. This can be partially overcome by utilizing substrate heating to quickly evaporate the solvent from the material as is done here by utilizing substrate temperatures of 30 or 40°C.

The layer thicknesses of the ink jetted films at different DPI's were measured by ellipsometry after UV curing and the values are shown in Figure 6. The layer thicknesses increases from 175 to 300 nm when increasing the DPI value from 450 to 600. This layer thickness already allows for a large range of structures to be imprinted. For the use in nanoimprinting, it is noteworthy that the droplet diameter of a single 2.4 pl droplet on the wafer is in the range of 100 µm or slightly less.

The ink jetting and optimal parameters needs to be still further tested on other types of printheads, for example on XAAR 1003 printhead. XAAR 1003 printhead utilizes also greyscale imprinting to adjust the layer thickness by having a range of droplet volumes ranging from 6 to 42 pl at native nozzle spacing of 360 npi.

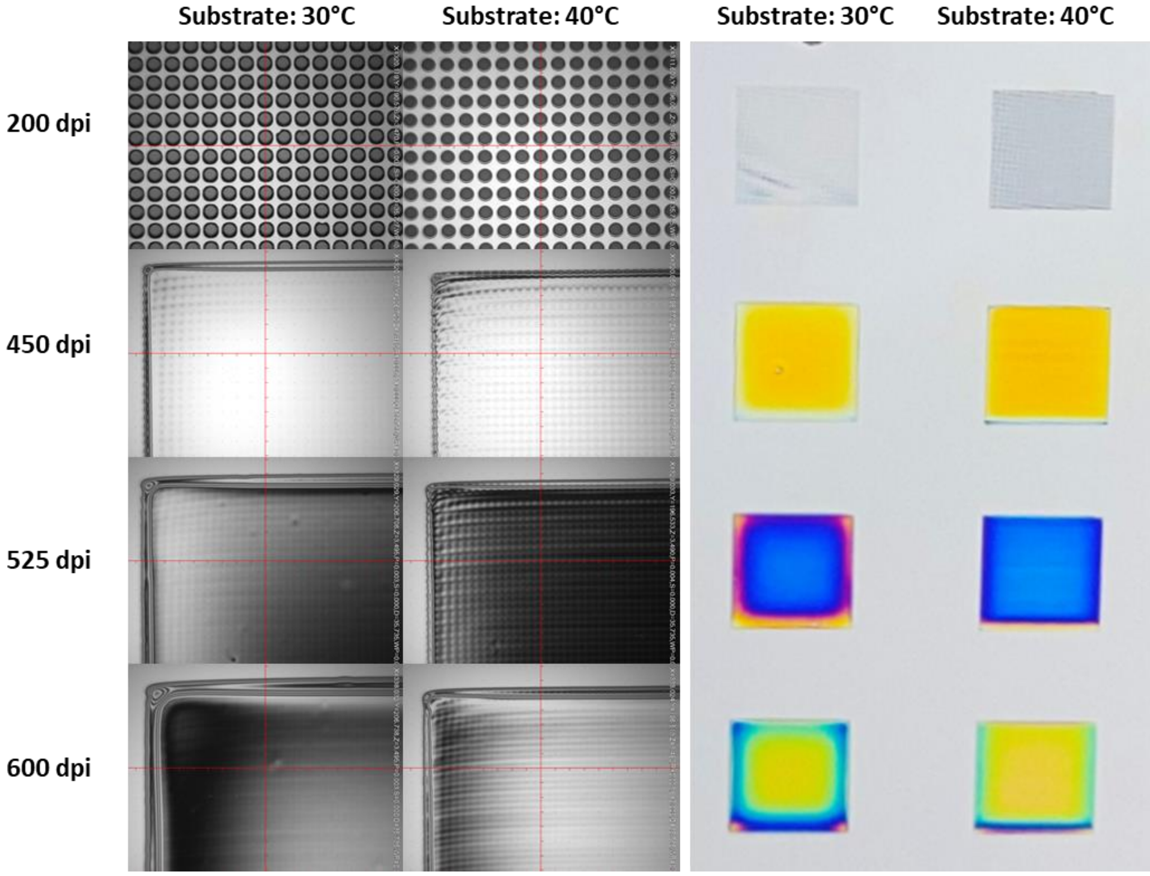

Figure 5. Examples of IPO-912 ink jetted with 2.4 pl cartridges with printhead temperature of 30°C. At low DPIs both substrate temperatures show a uniform array of droplets indicating stable ink jetting. The lower DPI settings show that a good uniformity can be reached by using substrate heating. At high DPI settings (600 dpi), the material will have a wet layer thickness that is so thick that the material starts to flow over larger distances upon solvent evaporation.

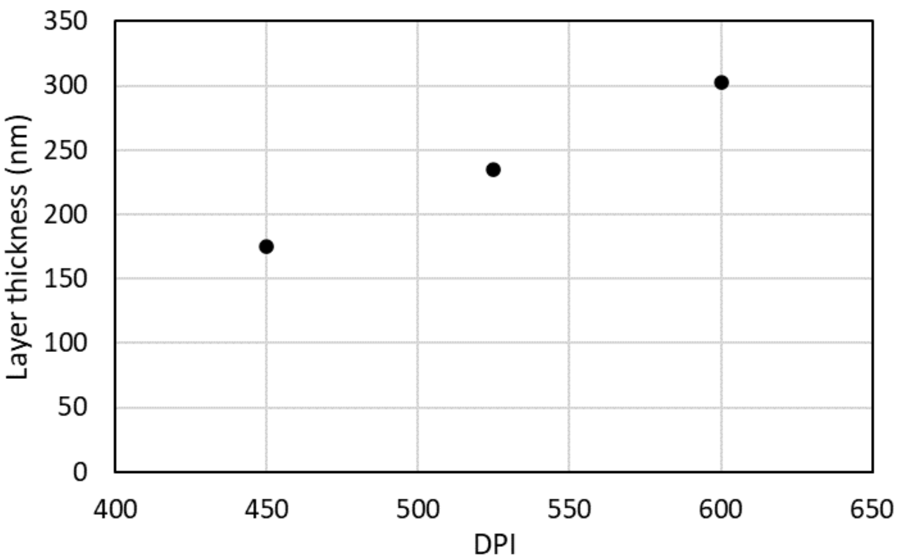

Figure 6. The layer thickness of cured film as a function of DPI with a 2.4 pl cartridge.

2.4. Nanoimprinting properties

The patternability of IPO-912 was tested first by imprinting the material deposited by spin coating. The imprint testing was done at Inkron facilities with an EVG7200 nanoimprinting system in SmartNIL mode. The general process is described in Table 2. The material is not designed for spin coating as an application method, and as a result the solvent system leads to poor thickness uniformity and non-optimal thickness. The imprinting of the prototype material IPO-912 was tested as is by imprinting a layer applied by spin coating, but a more detailed optimization of the imprintability of the formulation was done by using spin coating with a more conventional solvent system.

One key requirement for the nanoimprint materials is selective adhesion to the substrate with minimized adhesion to the working stamp material. Often this is solved by using an adhesion promoter, which is often applied by spin coating and a baking process. Good adhesion without adhesion promoter can be reached with conventional resin systems, but other restrictions can limit the possibilities of adjusting the formulation to optimize adhesion. This is the case with IPO-912, where currently ensuring good adhesion on a range of substrates requires an adhesion promoter. The recommended adhesion promoter for a spin coating process is Inkron product IAP-110, which is used here.

Figure 7 shows two AFM images of examples of imprinted line gratings with IPO-912 with spin coating as the deposition method. The spin coated layer thickness of the cured film was 730 nm. The smaller lines have 75 nm linewidth and height of 231 nm, which leads to an aspect ratio of ca. 3, showing that reasonably high aspect ratio lines can be imprinted with the resin. The features are broadened quite significantly by the AFM tip. The larger linewidth structures can also be imprinted with good pattern fidelity.

Table 2. The general imprinting process used for the imprint testing.

Substrate priming	IAP-110 adhesion promoter – spin coating 2000 rpm, 60s
Primer bake	150°C, 60s
Spin coating	2000 rpm, 120s
Pre-bake	80°C, 60s
Imprinting	EVG7200 in SmartNIL mode - EVG UV/AS2 as working stamp - 365 nm (UV-LED) cure (340 mW/cm2, 20 J)

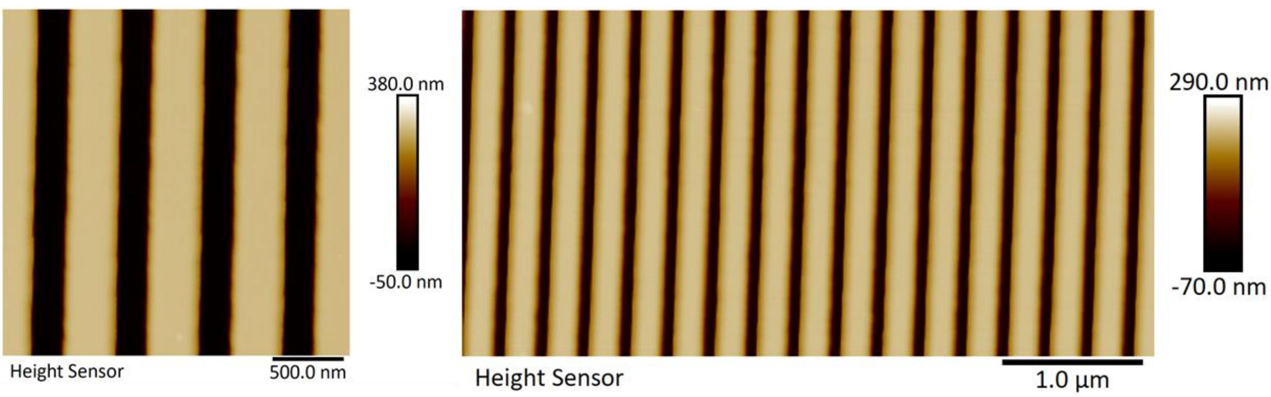

Figure 7. Examples of AFM images of imprinted structures. Left) Line grating with 600 nm period, 245 nm linewidth and 301 nm pattern height. Right) Line grating with 300 nm period, 75 nm linewidth and 231 nm pattern height.

For ease of testing, the improvements to the imprintability of the RI 1.9 formulation have been investigated by using spin coating as the application method. Therefore, the imprintability of a closely resembling resin and nanofiller system has been tested with spin coating as an application method for a wide range of structures. Figure 8 shows examples of line gratings that can be imprinted with the RI 1.9 resin. The structures show that various small and large linewidth structures can be imprinted with a good pattern fidelity into the spin coated films with relatively small residual layer thicknesses.

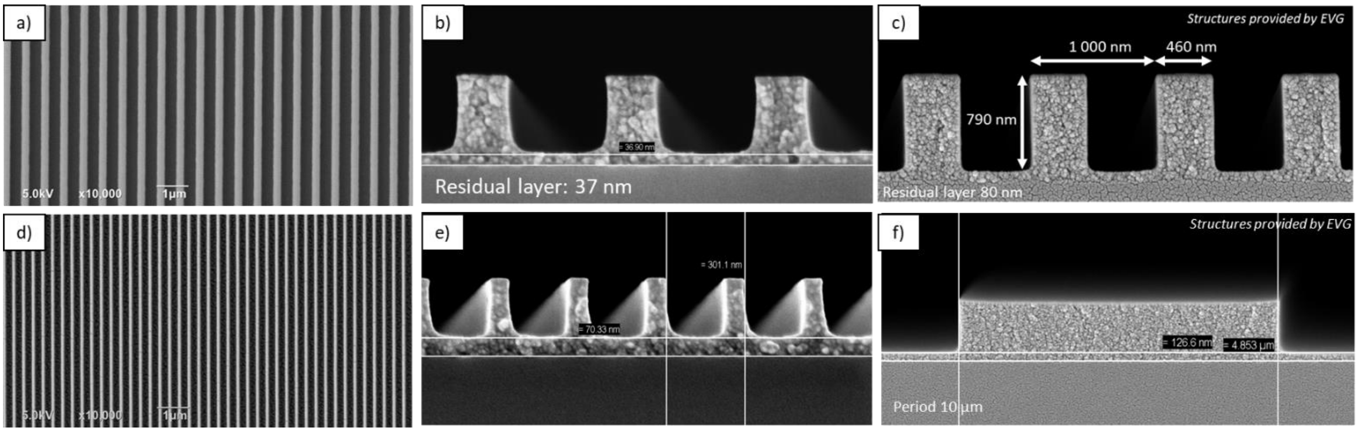

Figure 8. Examples of imprinted structures imprinted with a resin closely resembling IPO-912 except for the solvent system and additives. a & b) Line grating with period 600 nm, linewidth 245 nm and pattern height 301 nm. The structure is same as the structure in the Figure 7 (left); c) Line grating with 790 nm pattern height and 460 nm linewidth imprinted to a residual layer of 80 nm; d & e) Line grating with period 300 nm, linewidth 75 nm and pattern height 231 nm. The structure is same as the structure in the Figure 7 (right); f) Line grating with period of 10 µm and linewidth of 5 µm.

2.5. Combination of ink jet and nanoimprinting

The processing of IPO-912 by the combination of ink jetting and nanoimprinting is also demonstrated. As the ink jet testing is done on Dimatix DMC Samba 2.4 pl cartridges, to achieve a film thickness of around 200 nm in the imprinted film, the resist is ink jetted as a continuous film. The IPO-912 resist is ink jetted at 525 dpi with the substrate temperature set at 40°C onto an IAP-110 primed substrate. These specific conditions are also described in Figure 5.

The test pattern consists of a 5x5 array of squares of binary line and rectangular pillar gratings with 5 periodicities (300-800 nm) and two volume fillings in the line gratings. The height of the gratings is 100 nm. The structures are imprinted with a similar process as described in Table 2 except that the material deposition is done by ink jetting as was described above. Figure 9 shows images of the imprinted wafers, where the structures were successfully replicated. The material is deposited only at the grating areas. AFM images of the test structures are also shown in Figure 9. The roughness of the edges and in the surface arises from the master template.

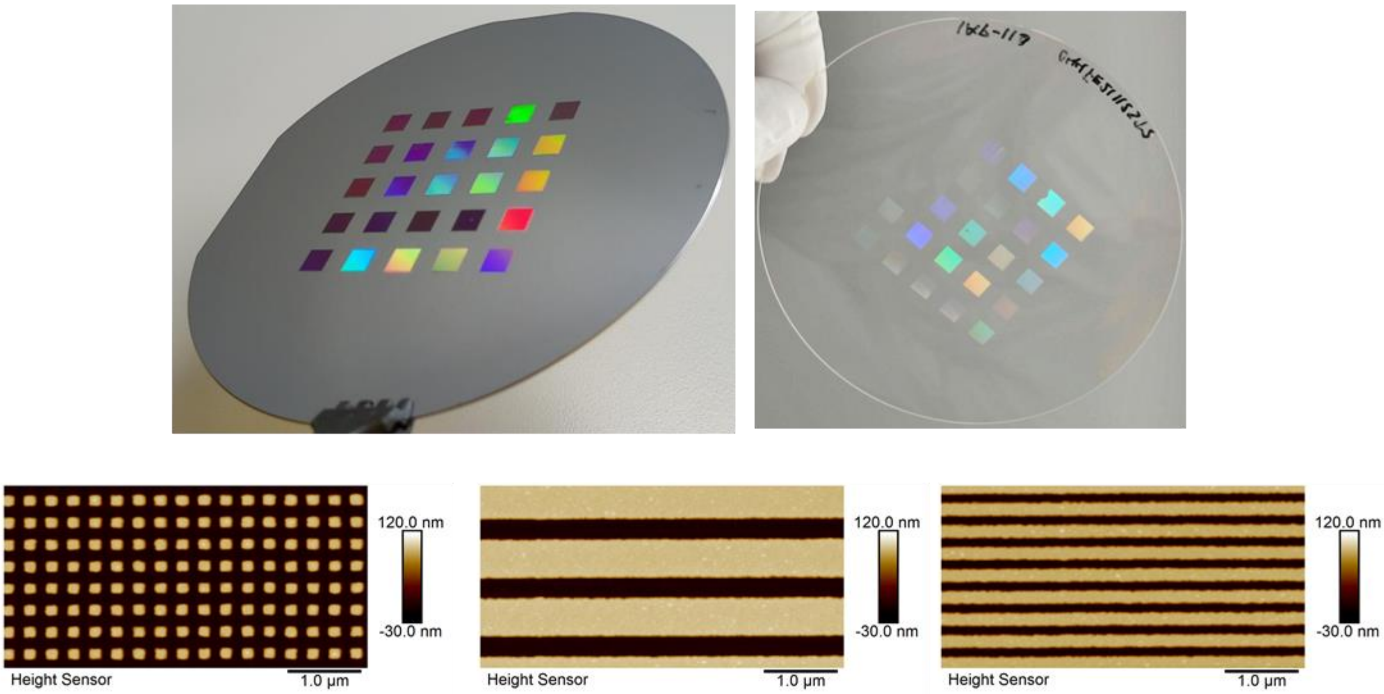

Figure 9. Top row) Nanoimprinted wafers (Si and RI 1.9 glass) of IPO-912 where the material has been deposited using ink jetting on PIXDRO LP50 and the structures have been imprinted using EVG7200 in SmartNIL mode. Bottom row) Examples of AFM images from the Si wafer. The line edge and surface roughness arise from the used stamp.

The results show that IPO-912 can be deposited by ink jetting and the deposited areas can be successfully imprinted. However, the imprintability of the ink jetted samples done by using various processing conditions needs to be further investigated. Especially the leveling of the resin layer over the length scale of tens of µm needs to be investigated. The IPO-912 base resist has a relatively high viscosity, which affects the leveling properties of the structures. This can be affected significantly with the processing conditions.

3. Conclusions

A prototype of an ink jet compatible refractive index (n_D) 1.9 nanoimprint resin was successfully developed. The properties of the developed prototype material were reported and discussed above. The resist meets the refractive index target and shows good optical properties also in the NIR range. The material shows a stable drop formation in ink jetting, and by adjusting the process conditions, a range of layer thicknesses can be reached with a reasonably good layer thickness uniformity. The combination of ink jetting and nanoimprinting is demonstrated with a layer thickness of 230 nm.

4. Outlook

As the following development steps, the prototype resist will be distributed to the respective consortium partners where further process testing will be executed to verify the performance of the resist. During development, the resist properties have been chosen to allow for modifications affecting the nanoimprintability and ink jet properties mostly separately. This allows for the material thickness control with different ink jet conditions, control of ink jet patternability and further improvement of the nanoimprinting and optical properties as development versions. In the subsequent development versions in the Task 5.7 especially adhesion, thickness uniformity of the ink jetted layer and resin flowability are addressed.

5. Degree of Progress

The DoA assigns the deliverable as a high refractive index material prototype for OPA application based on the definitions in D2.2 and D2.5. The definitions for the prototype material from deliverables D2.2 and D2.5 were successfully fulfilled. The use of the material for imprinting the features required by the OPA application remains to be tested.